Sorting out Semiconducting Single-Walled Carbon Nanotube Arrays by Washing off Metallic Tubes Using SDS Aqueous Solution

*Yue Hu, Yabin Chen, Pan Li, and Jin Zhang**

Single-walled carbon nanotubes (SWNTs) have been regarded as one of the best candidates for future application in next generation integrated circuits due to their unique structures and superb properties.[1–6] However, SWNTs produced by almost all of the current available approaches are always mixtures of metallic (*m*-) and semiconducting (*s*-) SWNTs, normally containing about 1/3 *m*-SWNTs. This coexistence of *m*- and *s*- SWNTs sample will dramatically decrease the performance of devices. Meanwhile, parallel *s*-SWNTs are necessary to enable high-current and high-speed nanotube FETs to surpass modern silicon devices.[7] Thus, high density *s*-SWNT arrays with well alignment are highly desirable.

During the past decades, several approaches have been developed to produce *s*-SWNTs, such as solution-phase separation of *m*-SWNTs and *s*-SWNTs, selective destruction of *m*-SWNTs, and selective growth of *s*-SWNTs. For the solution-based separation, density-gradient-inducing centrifugation[8] could enable the optimal isolation of a targeted electronic type or a specific chirality of SWNT. Agarose-gel-based separation,[9] dielectrophoresis,[10] and DNA-SWNT hybrid[11] all could achieve the enrichment of *s*-/*m*- SWNTs. However, most of these separation methods, which involve complicated physical and/or chemical processes, inevitably brought contamination, and also the separated tubes were very short and in random orientation. In the case of selective destruction of *m*-SWNTs, such as nitronium ion attack,[12] gas-phase plasma etching,[7] and water preferential destruction,[13] by which we could also get *s*-SWNTs. But they might 'miskill' the small-diameter *s*-SWNTs and at the same time *m*-SWNTs of large diameter couldn't be etched by the plasma. As to the selective growth of *s*-SWNTs approach, for instance, plasma enhanced growth,[14] in situ ultraviolet irradiation[15] and methanol-assisted growth,[16] could provide *s*-SWNT arrays. But their mechanisms were not clear. Therefore, how to obtain well aligned *s*-SWNT arrays with high density and perfect structures still remains a big challenge.

Surfactant-assisted decontamination is a widely used method to remove contaminant because of the difference between interactions of the contaminant and surfactant and that between contaminant and the surface. Inspired by this idea, if there is a type of surfactant, which has stronger interaction with *m*-SWNTs as compared to the counterpart *s*-SWNTs, then the *m*-SWNTs would be washed off while the *s*-SWNTs remain on surface. Thus, how to select appropriate surfactants or molecules possessed preferentially interaction with *m*-SWNTs is the key issue. Based on the electron density difference of *m*-SWNTs and *s*-SWNTs, Bao and co-workers selectively aligned *m*-SWNTs and *s*-SWNTs onto amine-terminated and phenyl-terminated silane treated surfaces, respectively.[17] In our recent work, the 'Scotch Tape' separation method[18] was developed which was due to phenyl functional groups can selectively adsorb on *m*-SWNTs while amine functional groups prefer *s*-SWNTs. Along with these work, several efforts also have been carried out to separate *m*-SWNTs and *s*-SWNTs using the selective adsorption of surfactant. For example, sodium dodecyl sulfate (SDS), sodium cholate hydrate, sodium deoxycholate monohydrate, and sodium dodecylbenzene sulfonate have been used for *s*-/*m*- SWNTs separation.[19] SDS is most frequently used due to the significant difference of interaction between SDS and *s*-/*m*- SWNTs. It was reported that the SWNTs could be sorted by both electronic type and diameter by optimizing SDS assisted elution condition.[20] Recently, large-scale single-chirality separation of SWNTs was achieved by a single-surfactant multicolumn gel chromatography method.[21] However, the direct evidence that the SDS molecules could selectively adsorb on *m*-SWNTs has not been obtained.

In the present study, we reported a simple procedure to sort out the *s*-SWNT arrays on ST-cut quartz surface by washing off *m*-SWNTs using SDS aqueous solution with assistance of ultrasonication. We directly observed that SDS molecules selectively adsorb on *m*-SWNTs, and following ultrasonic treatment enabled elution of *m*-SWNTs and getting well aligned *s*-SWNT arrays. The well aligned individual

Y. Hu, Y. B. Chen, P. Li, Prof. J. Zhang
Center for Nanochemistry
Beijing National Laboratory for Molecular Sciences
Key Laboratory for the Physics and
Chemistry of Nanodevices
State Key Laboratory for Structural Chemistry
of Unstable and Stable Species
College of Chemistry and Molecular Engineering
Peking University
Beijing 100871, PR China
E-mail: jinzhang@pku.edu.cn

DOI: 10.1002/smll.201202940

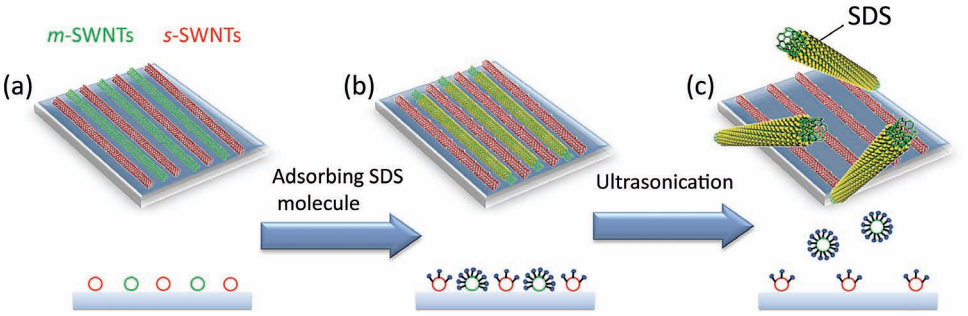

Figure 1. Schematic illustration of sorting out *s*-SWNT arrays on surface by washing off the *m*-SWNTs using SDS aqueous solution.

SWNT arrays were firstly grown on ST-cut quartz surface with mixture of *m*- and *s*-SWNTs (**Figure 1** a). The quartz substrate was then immerged into the SDS aqueous solution and the SDS molecules could preferentially adsorb on *m*-SWNTs (Figure 1b). Analogous to the process of decontamination, the *m*-SWNTs covered with SDS molecules were easier to enter into solutions with assistance of ultrasonication while the *s*-SWNTs still remained on the substrate (Figure 1c).

Figure 2 shows the typical scanning electron micoroscope (SEM) image, atomic force microscope (AFM) image, and Raman spectra of the as-grown SWNT arrays. SEM image (Figure 2a) indicates that the SWNT arrays are uniform over larger area. The AFM image (Figure 2b) shows the average density of SWNTs on quartz surface is about 3-4 tubes per μm and the average diameter of the SWNTs is about 1.1 nm (Figure 2c). The Raman spectra (Figure 2d) of the SWNT arrays transferred onto SiO_2/Si substrate with 514.5 nm excitation indicates that the tubes are mixture of *m*-SWNTs and *s*-SWNTs according to the Kataura plot.[22] We have detected 518 RBM signals of as-grown SWNTs and among them 358 were from *s*-SWNTs (Figure 2d). The percentage of s-SWNTs is ~69.1% and the ratio of *m*-SWNTs to *s*-SWNTs is nearly 1 to 2.

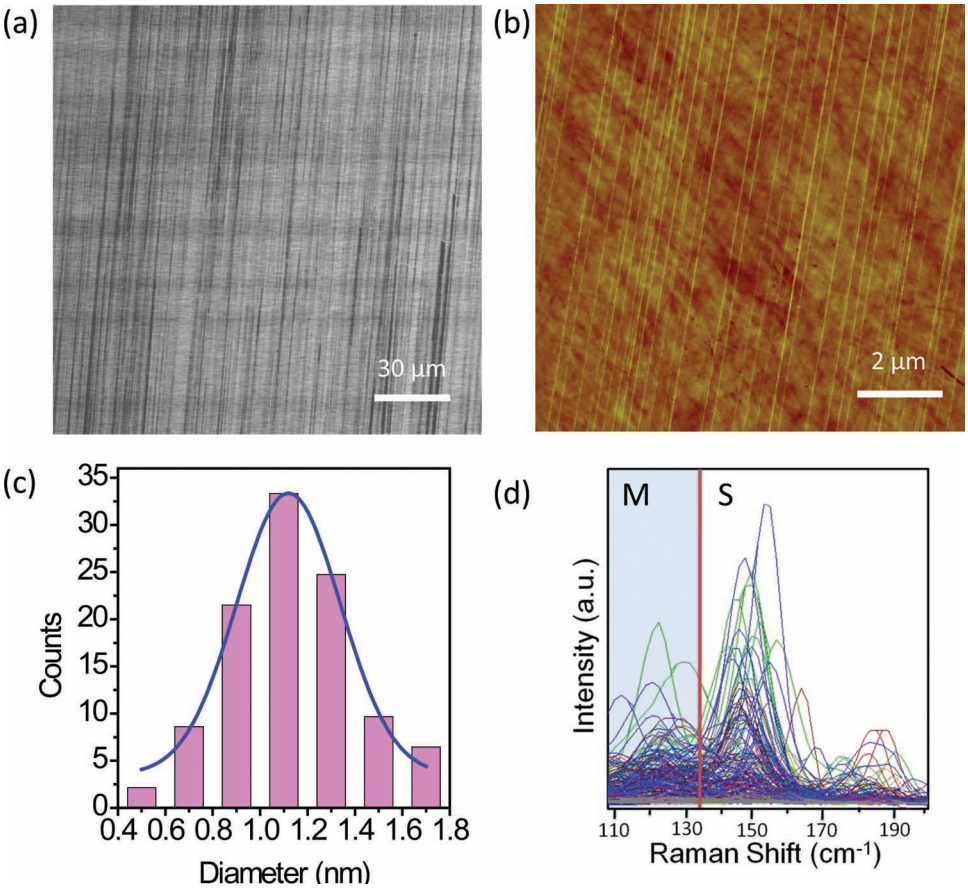

Figure 2. (a,b) SEM and AFM images of the as-grown SWNT arrays on quartz surface. (c) Diameter distribution of the as-grown SWNTs. (d) Raman spectra of the as-grown SWNT arrays transferred onto SiO_2/Si substrate with 514.5 nm excitation.

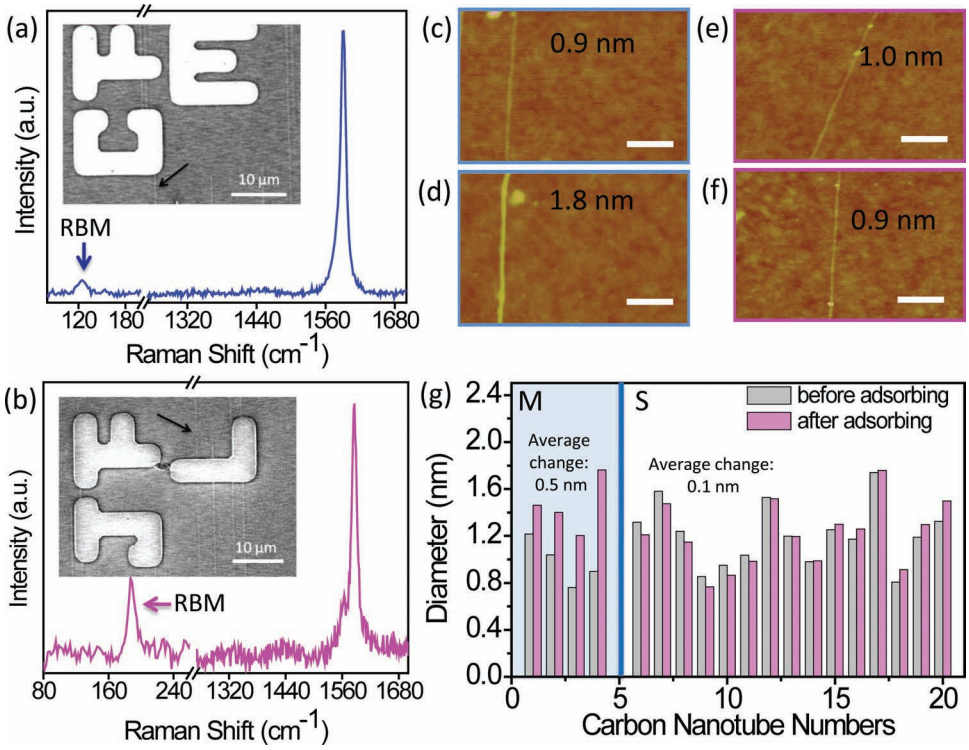

Figure 3. (a,b) Raman spectra of SWNTs pointed by the black arrow in the corresponding insert SEM image with 514.5 nm excitation. (c,d) AFM images of the *m*-SWNT in (a) before (c: 0.9 nm) and after (d: 1.8 nm) adsorbing SDS molecules. (e,f) AFM images of the *s*-SWNT in (b) before (e: 1.0 nm) and after (f: 0.9 nm) adsorbing SDS molecules. (g) Statistical result of *m*-SWNT and *s*-SWNT diameters before and after adsorbing SDS molecules. The scale bars of AFM images are 150 nm.

These mixtures of *m*- and *s*- SWNTs were used as samples for 'wash-off' separation. After ultrasonication in SDS aqueous solution, some SWNTs disappeared while the others still remained on the substrate. Based on the phenomenon, we speculated that the SDS molecules might selectively adsorb on *m*-SWNTs and thus the *m*-SWNTs would be preferentially washed off. In order to get the direct evidence, the as-grown SWNTs were firstly transferred onto SiO_2/Si substrates by applying the peel-off method[23] for Raman characterization. And then AFM was used to directly measure the diameters of SWNTs before and after adsorbing SDS molecules. **Figure 3** a and b are typical Raman spectra with 514.5 nm excitation for the black arrow pointed SWNT in the corresponding insert SEM images. According to the Raman shift of RBM, the pointed (by black arrow) tube in (a) is *m*-SWNT while (b) is *s*-SWNT. With the help of the marks in SEM images (the insets of Figure 3a,b), we could precise fix the position of the SWNTs and measure their diameters by AFM. Figure 3c–f are typical AFM images of *m*-SWNTs and *s*-SWNTs diameters before and after adsorbing SDS molecules. It is found that the diameter of *m*-SWNT becomes 0.9 nm larger after adsorbing SDS molecules while the diameter of *s*-SWNT is almost unchanged. After measuring nearly 20 tubes, statistical result (Figure 3g) indicates that the average diameter variation of *m*-SWNTs is about 0.5 nm, while that is just 0.1 nm for *s*-SWNTs. Thus, we could come to the conclusion that SDS molecule would selectively adsorb on *m*-SWNTs, and thus the *m*-SWNTs can be washed off.

There has been quite a bit of research into the mechanism of the interaction between SDS and SWNTs. It was reported that the morphology and coverage of SDS coating on SWNTs was dependent on the SWNTs structures.[24,25] There are about three morphologies that surfactants self-assemble on SWNTs. The first one is that the SDS molecules perpendicularly adsorbed on the surface of SWNTs forming a monolayer. It looks like the SWNT in a cylindrical SDS micelle.[26] The second type is the SDS molecules would be organized into half cylinders adsorbed on SWNTs surface.[27] And the last one is the SDS molecules are random adsorbed on SWNTs.[28] Furthermore, *m*-SWNTs are generally thought to be fully covered by SDS.[9] Combining with our experimental results, we speculate that *m*-SWNTs are in a cylindrical SDS micelle while SDS molecules are random adsorbed horizontal on *s*-SWNTs. However, the length of SDS molecule is over 2 nm and if SDS molecules adsorb perpendicularly to the surface of the *m*-SWNTs, the *m*-SWNTs diameter change should be more than 2 nm. In fact, it is obvious that SDS micelle only exists in SDS aqueous solution. And before measuring the diameter, the SWNTs samples adsorbed with SDS molecules were blown dry by high purity nitrogen. This process might cause the morphology of SDS changing, from perpendicular to have an angle with SWNTs surface. Therefore, the diameter change of *m*-SWNTs before and after SDS adsorption in our experiment is about 0.5 nm.

For directly washing off *m*-SWNTs from horizontally aligned nanotube arrays on quartz surface, we also measured the diameters of as-grown SWNTs on quartz substrates

small NANO MICRO

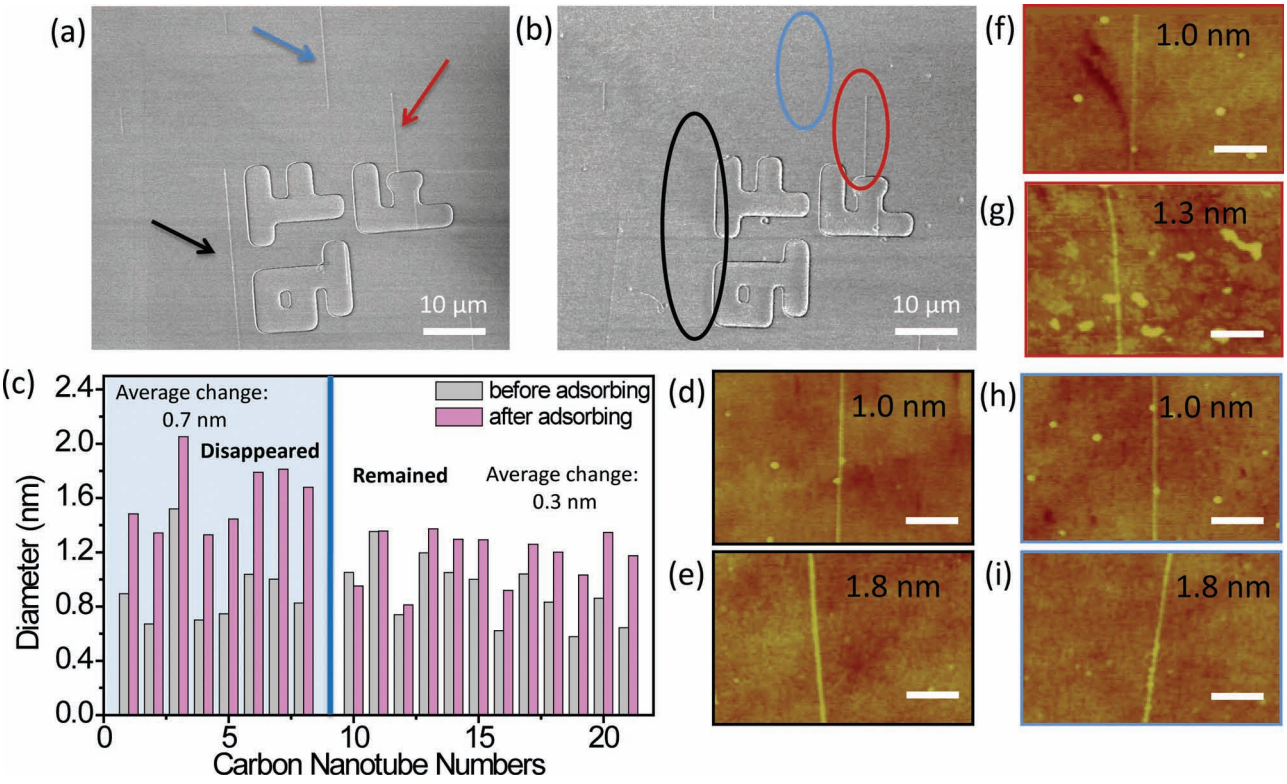

Figure 4. (a,b) SEM images of SWNTs on quartz surface before and after separation, respectively. (c) Statistical result of disappeared SWNTs and remained SWNTs diameters before and after adsorbing SDS molecules. (d–i) AFM images of the SWNTs in (a) before (d,f,h) and after (e,g,i) adsorbing SDS molecules pointed by black (d,e), red (f,g), and blue (h,i) arrows. The scale bars of AFM images are 150 nm.

before (**Figure 4** d,f,h) and after (Figure 4e,g,i) adsorbing SDS molecules, respectively. As shown in Figure 4a, the diameters of SWNTs pointed by black and blue arrows are both getting 0.8 nm larger after adsorbing SDS molecules, while the red arrow pointed SWNT diameter is only getting 0.3 nm larger after adsorbing. According to the above results, we believe the SWNTs pointed by black and blue arrows are *m*-SWNTs and which pointed by the red arrow are *s*-SWNT. After ultrasonication, the SWNTs in black and blue rings disappear while the SWNT in red ring remains on quartz substrate (Figure 4b). It means that *m*-SWNTs are washed off and the *s*-SWNT remains. After measuring more than 20 tubes, statistical result (Figure 4c) indicates that the SWNTs with bigger average diameter changes (about 0.7 nm, considered as *m*-SWNTs) are mostly disappeared after separation while SWNTs with smaller average diameter changes (about 0.3 nm, considered as *s*-SWNTs) remain on quartz substrate. Therefore, we could obtain *s*-SWNT arrays on quartz surface by this 'wash-off' separation method.

Furthermore, we used this method to separate SWNT arrays with larger area on quartz substrate directly. In order to achieve better separation performance, different experiment parameters, such as concentration of SDS aqueous solution, time and power of ultrasonication were considered and optimized for washing off *m*-SWNTs. It was found that long time and high power of ultrasonication using high concentration of SDS aqueous solution would wash off all the SWNTs on quartz substrate while nearly no SWNTs decreased under short time and low power of ultrasonication using low concentration of SDS aqueous solution. After dozens of attempts, we found from SEM images that about 1/3 SWNTs were washed off when the ultrasonication power was 40%, the ultrasonication time was about 20 min and concentration of SDS aqueous solution was about 2% by mass. This ratio was comparable with the 1/3 *m*-SWNTs in as-grown SWNTs obtained from general growth methods. As shown in **Figure 5**a,b, it is obvious that about 1/3 SWNTs were washed off after separation in the same region. Then we transferred the separated SWNTs on quartz substrates onto SiO_2/Si substrates for Raman characterization. 139 RBM signals of the SWNTs were detected and among them 126 were *s*-SWNTs (Figure 5c). So the percentage of *s*-SWNTs is ~90.6%. It means that almost all of *m*-SWNTs signals were disappeared and over 90% of *s*-SWNTs in the arrays were left on substrate.

To further confirm these results, SWNT samples were also characterized by electrical characteristics. SWNT arrays treated under the best conditions were transferred onto SiO_2/Si substrates with 300 nm SiO_2 by applying the peel-off method to fabricate back gate field effect transistors (FET). Electron beam lithography (EBL) was used to identify electrode structures and location. The source and drain electrodes were made by Ti (5 nm)/Pd (45 nm). As shown in Figure 5d,e, FET devices with a channel length of 2.5 μm containing dozens of SWNTs in the channel region were fabricated. Transfer characteristics of FET devices were

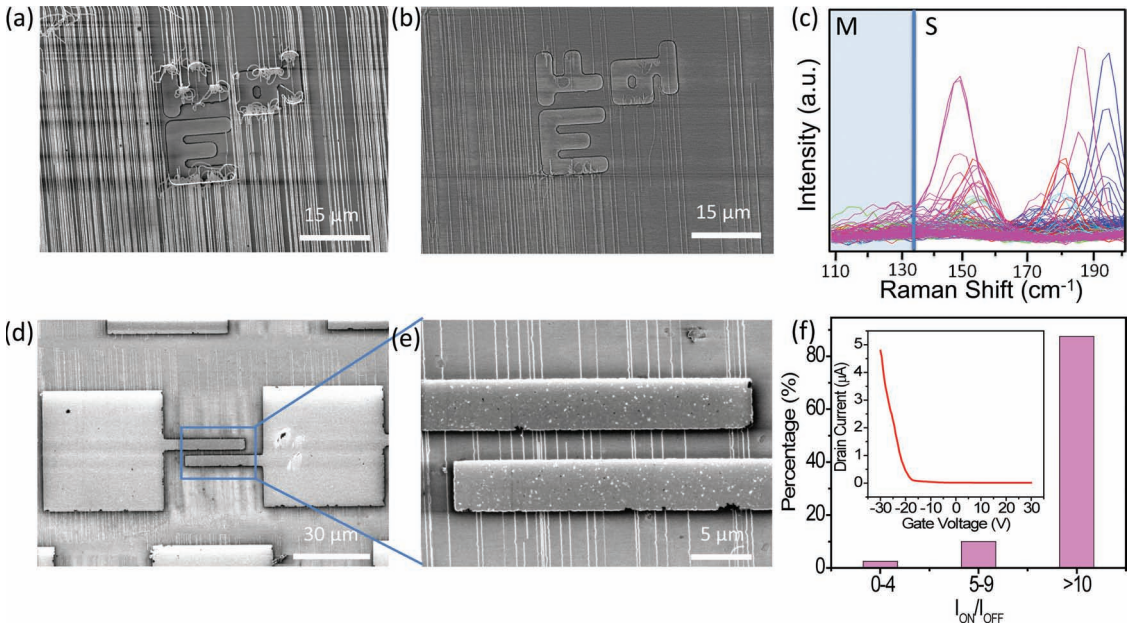

Figure 5. (a,b) SEM images of SWNT arrays on quartz surface before and after separation. (c) Raman spectra with 514.5 nm excitation of SWNT arrays transferred onto SiO_2/Si substrate after separation. (d,e) SEM images of an FET device fabricated by *s*-SWNT arrays. (f) Distribution of *s*-SWNTs FET devices according to their I_{on}/I_{off} ratios. (The inset in (f) is a typical transfer characteristic curve of *s*-SWNTs device with V_{ds} = 100 mV).

measured under a bias voltage V_{ds} = 100 mV in air at room temperature. The insert in Figure 5f shows a typical I_{ds}-V_g curve of our FET constructed by the *s*-SWNT arrays. In particular, the I_{on}/I_{off} ratio of 10 is expected if 90% of tubes are semiconducting assuming all SWNTs have similar resistances in their ON-state. The statistical result of transport behavior of 40 FET devices shows that nearly 90% devices' I_{on}/I_{off} ratios were more than 10 (Figure 5f). It means that the percentage of *s*-SWNTs can be higher than 90% to some extent. Because of the space limitation, here we only present three typical device transfer curves (Figure S1a) and all device on/off ratios (Figure S1b).

At last, a mechanism was supposed for the *s*-/*m*- SWNTs separation. We confirmed that SDS micelle formation would decrease the tube-substrate interaction (Figure S2). The differences in the surface electron states of *s*-/*m*- SWNTs affect the interaction between SWNTs and SDS. Thus, the morphology and coverage of SDS coatings on *s*-/*m*- SWNTs is different. SDS coating fully covering the *m*-SWTNs minimizes their interactions with quartz substrates while the *s*-SWNTs interactions with substrates nearly don't decrease. After ultrasonication with appropriate experiment parameters, the *m*-SWNTs could be easily washed off while the *s*-SWNTs still remain on the substrate. In addition, we found there is no selective separation of *s*-/*m*- SWNTs by diameter in our experiment.

In summary, a facile and effective strategy for sorting out the *s*-SWNT arrays on surface by washing off the *m*-SWNTs using SDS aqueous solution was developed. We could selectively remove the *m*-SWNTs from horizontally aligned nanotube arrays using SDS aqueous solution. Long and high quality horizontally aligned SWNT arrays with over 90% *s*-SWNTs were obtained by this method. In addition, it should be noted that the method is simple, low cost, and easily scalable to a large quantity separation process. It would be convenient for future *s*-SWNTs device applications. By the way, if there are other surfactants which have stronger interaction with *s*-SWNTs, in use of the 'wash-off' separation method, *m*-SWNT arrays also might be obtained.

Experimental Section

The ST-cut quartz (miscut angle <0.5°) obtained from Hefei Kejing Materials Technology Co., China was used as substrates to grow SWNT arrays. After cleaning, the quartz substrates were annealed at 900 °C in air for 8 hours. Then 0.05 mM $Fe(OH)_3$/ethanol solution was patterned onto the quartz surface by "Needle-Scratching"[29] as catalysts. The SWNT growth was carried out in a home-made chemical vapor deposition (CVD) system (the diameter of the quartz tube is 1 inch). After heating the substrate to 830 °C in air, 300 standard cubic centimeters per minute (sccm) argon and 300 sccm H_2 were introduced for 10 min to reduce the catalysts. Finally, 10 sccm Ar was bubbled through ethanol for 20 min to grow the SWNT arrays. The quartz substrate with as-grown SWNT arrays was directly immerged into the SDS (99%, Sigma-Aldrich) aqueous solution. After ultraconication (Scientz SB-5200DTDN, 300 W, 40 kHz) with certain minutes, the quartz substrates with SWNTs were rinsed with a large amount of deionized water for several times to wash off *m*-SWNTs and excess SDS molecules. Tapping-mode AFM (NanoScope IIIa, Veeco Co., USA), Scanning electron microscopy (SEM, Hitachi S4800, Japan), Raman spectroscopy (Horiba HR800 Raman system) and Keithley 4200-SCS Semiconductor Characterization System were used to characterize the structures and properties of SWNTs.

small NANO MICRO

Supporting Information

Supporting Information is available from the Wiley Online Library or from the author.

Acknowledgements

This work was supported by NSFC (51272006, 21129001, 21233001, and 51121091) and MOST (2011CB932601).

[1] M. S. P. Shaffer, A. H. Windle, *Adv. Mater.* **1999**, *11*, 937–941.
[2] M. Cadek, J. N. Coleman, V. Barron, K. Hedicke, W. J. Blau, *Appl. Phys. Lett.* **2002**, *81*, 5123–5125.
[3] B. Vigolo, P. Poulin, M. Lucas, P. Launois, P. Bernier, *Appl. Phys. Lett.* **2002**, *81*, 1210–1212.
[4] J. E. Peters, D. V. Papavassiliou, B. P. Grady, *Macromolecules* **2008**, *41*, 7274–7277.
[5] S. J. Kang, C. Kocabas, T. Ozel, M. Shim, N. Pimparkar, M. A. Alam, S. V. Rotkin, J. A. Rogers, *Nat. Nanotechnol.* **2007**, *2*, 230–236.
[6] A. D. Franklin, M. Luisier, S. J. Han, G. Tulevski, C. M. Breslin, L. Gignac, M. S. Lundstrom, W. Haensch, *Nano Lett.* **2012**, *12*, 758–762.
[7] G. Y. Zhang, P. F. Qi, X. R. Wang, Y. R. Lu, X. L. Li, R. Tu, S. Bangsaruntip, D. Mann, L. Zhang, H. J. Dai, *Science* **2006**, *314*, 974–977.
[8] M. S. Arnold, A. A. Green, J. F. Hulvat, S. I. Stupp, M. C. Hersam, *Nat. Nanotechnol.* **2006**, *1*, 60–65.
[9] T. Tanaka, H. Jin, Y. Miyata, S. Fujii, H. Suga, Y. Naitoh, T. Minari, T. Miyadera, K. Tsukagoshi, H. Kataura, *Nano Lett.* **2009**, *9*, 1497–1500.
[10] R. Krupke, F. Hennrich, H. von Lohneysen, M. M. Kappes, *Science* **2003**, *301*, 344–347.
[11] M. Zheng, A. Jagota, M. S. Strano, A. P. Santos, P. Barone, S. G. Chou, B. A. Diner, M. S. Dresselhaus, R. S. McLean, G. B. Onoa, G. G. Samsonidze, E. D. Semke, M. Usrey, D. J. Walls, *Science* **2003**, *302*, 1545–1548
[12] K. H. An, J. S. Park, C. M. Yang, S. Y. Jeong, S. C. Lim, C. Kang, J. H. Son, M. S. Jeong, Y. H. Lee, *J. Am. Chem. Soc.* **2005**, *127*, 5196–5203.
[13] P. Li, J. Zhang, *J. Mater. Chem.* **2011**, *21*, 11815.
[14] Y. M. Li, D. Mann, M. Rolandi, W. Kim, A. Ural, S. Hung, A. Javey, J. Cao, D. W. Wang, E. Yenilmez, Q. Wang, J. F. Gibbons, Y. Nishi, H. J. Dai, *Nano Lett.* **2004**, *4*, 317–321.
[15] G. Hong, B. Zhang, B. H. Peng, J. Zhang, W. M. Choi, J. Y. Choi, J. M. Kim, Z. F. Liu, *J. Am. Chem. Soc.* **2009**, *131*, 14642–14643.
[16] L. Ding, A. Tselev, J. Y. Wang, D. N. Yuan, H. B. Chu, T. P. McNicholas, Y. Li, J. Liu, *Nano Lett.* **2009**, *9*, 800–805.
[17] M. C. LeMieux, M. Roberts, S. Barman, Y. W. Jin, J. M. Kim, Z. Bao, *Science* **2008**, *321*, 101–104.
[18] G. Hong, M. Zhou, R. Zhang, S. Hou, W. Choi, Y. S. Woo, J. Y. Choi, Z. Liu, J. Zhang, *Angew. Chem. Int. Ed.* **2011**, *50*, 6819–6823.
[19] T. Tanaka, H. Jin, Y. Miyata, H. Kataura, *Appl. Phys. Express* **2008**, *1*, 114001.
[20] H. Gui, H. Li, F. Tan, H. Jin, J. Zhang, Q. Li, *Carbon* **2012**, *50*, 332–335.
[21] H. Liu, D. Nishide, T. Tanaka, H. Kataura, *Nat. Commun.* **2011**, *2*, 309.
[22] A. Jorio, R. Saito, J. Hafner, C. Lieber, M. Hunter, T. McClure, G. Dresselhaus, M. Dresselhaus, *Phys. Rev. Lett.* **2001**, *86*, 1118–1121.
[23] L. Y. Jiao, X. J. Xian, Z. Y. Wu, J. Zhang, Z. F. Liu, *Nano Lett.* **2009**, *9*, 205–209.
[24] Z. Xu, X. Yang, Z. Yang, *Nano Lett.* **2010**, *10*, 985–991.
[25] N. R. Tummala, A. Striolo, *ACS Nano* **2009**, *3*, 595–602.
[26] M. J. O'Connell, S. M. Bachilo, C. B. Huffman, V. C. Moore, M. S. Strano, E. H. Haroz, K. L. Rialon, P. J. Boul, W. H. Noon, C. Kittrell, J. Ma, R. H. Hauge, R. B. Weisman, R. E. Smalley, *Science* **2002**, *297*, 593–596.
[27] C. Richard, F. Balavoine, P. Schultz, T. W. Ebbesen, C. Mioskowski, *Science* **2003**, *300*, 775–778.
[28] K. Yurekli, C. A. Mitchell, R. Krishnamoorti, *J. Am. Chem. Soc.* **2004**, *126*, 9902–9903.
[29] B. Li, X. Cao, X. Huang, G. Lu, Y. Huang, C. F. Goh, F. Y. Boey, H. Zhang, *Small* **2009**, *5*, 2061–2065.

Received: November 26, 2012
Revised: January 7, 2013
Published online: March 18, 2013

